24th COBEM - 2017

24th ABCM International Congress of Mechanical Engineering
December 3-8, 2017, Curitiba, PR, Brazil

COBEM-2017-2042
EXPERIMENTAL STUDY OF PENETRATION DEPTH PRODUCED BY A PLUNGING JET SYSTEM

Pedro José Miranda-Lugo
Douglas Ricardo Sansão
L. Enrique Ortiz-Vidal
Oscar M. H. Rodriguez
Industrial Multiphase Flow Laboratory (LEMI), Mechanical Engineering Department, São Carlos School of Engineering, University of São Paulo (USP), São Carlos, SP, Brazil.
e-mail: pjosemiranda@usp.br
e-mail: Douglas.sansao@usp.br
e-mail: leortiz@sc.usp.br
e-mail: oscarmhr@sc.usp.br

Abstract. *It was studied the phenomenon of air entrainment and depth penetration reached by the air entrained by a vertical plunging jet system. Breaking and coalescence bubbles process were also study by an optical technique to understand the kinetic energy dissipation. An experimental setup was designed and constructed in order to carry out a set of experiments using water like working fluid. We tested different liquid flow with various Nozzle heights. The plunging jet nozzle was carefully designed to ensure a fully developed turbulent velocity profile inside it. A high-speed camera was used to film air entrainment flow induced by a water jet impacting a stagnated surface in a transparent acrylic reservoir with a water volume previously chosen. The experimental results showed greater penetration depths with greatest water flow and lowest Nozzle heights. Furthermore, we noticed that both the higher Nozzle height and the greater liquid flow, the more air entrainment. The results obtained are in agreement with data reported in the literature.*

Keywords: *air entrainment, penetration depth, plunging jet, image processing.*

1. INTRODUCTION

Many environmental and industrial processes, such as breaking waves in the sea, aeration of chemical reactions, spillage of liquids into containers, the stirring of a molten liquid phase, involve complex two-phase flows, generated by the air entrainment produced when a liquid of the same or different properties impacts over a free surface (Biń, 1993) and (Chanson, 1992). This process can be better understood with a very common phenomena called in the literature as *plunging jet systems*. It is observed when a liquid jet plunges into a free liquid surface after passing through a gaseous phase surrounding, draging a quantity of gas into the receiving pool and creating a region of two submerged phases (Harby *et al.*, 2014; Qu *et al.*, 2011) and (Roy *et al.*, 2013). The interfacial area of this region influence directly on the design of equipment for the industry and the development of new technologies for process optimization.

Several researchers, (Biń, 1993; Bonetto and Lahey, 1993; Brattberg and Chanson, 1998) and (Chanson and Brattberg, 2000), studied air entrainment due to plunging jets, revealing some specific characteristics of the air-water flows induced by the jets. According to Ohkawa *et al.* (1987), previous authors adopted four operational variables that affect the gas entrainment characteristics of a liquid jet: nozzle diameter (D_n), output velocity of the nozzle (V_n), nozzle height (H_n) and the nozzle angle respect to vertical axis (β). Other important factors are the nozzle design, specifically the length-diameter ratio $\left(\frac{L_n}{D_n}\right)$, the physical fluids properties, meanly of viscosity (μ) and surface tension (σ), and the jet turbulence (Tu) (Burgess and Molloy, 1973; Biń, 1993; Cummings and Chanson, 1997). Furthermore, conforming to Qu *et al.* (2013), the air entrainment under a stagnant liquid is also controlled by the topology of the jet surface before the impact, related to jet turbulence, and the complex movement induced on the stagnant liquid during impact.

Nowadays, various optical techniques to determine particles size are available in the biography. One of the main *in-situ* techniques of particle size measurement are the methods based on images recognition. According to Maaß *et al.* (2008), these provided accurate particle size values in the analyzed system. Direct image technique is an effective and convenient method to estimating of the particle size distribution (Maaß *et al.*, 2008; Zhang *et al.*, 2012). The literature reported different types of experimental techniques based on filming to recognizing elements, being the simplest the planar image technique, which uses a high speed camera to film the particles of interest. In case of deformation and sudden oscillations, authors recommend the use of either two or three cameras, as reported by Hassan *et al.* (2001); Celata *et al.* (2006) and

Bröder and Sommerfeld (2007). A complementary technique widely used together the first one is the *Shadow Sizing*. This consist of using a backlight so that the particle or bubbles, if gas-liquid flow, appear darkened in the image with a greater contrast, making the further processing of the image less susceptible to errors (Said, 2011).

In order to study the penetration depth of the air entrainment below a stagnant liquid surface due to a water jet, it was performed an experimental work using a plunging jet system. An algorithm with image processing techniques was designed in MatLab and used to determine the mean penetration depth of the air entrained.

2. EXPERIMENTAL WORK

2.1 Experimental setup

In order to study the phenomenon of air entrainment produced by a plunging jet system through *Shadow Sizing* technique, the experimental facility shown in Figure 1 was built at LEMI-EESC-USP. This consists of two water reservoirs connected through a flexible tubing of 5 cm in diameter, where the Reservoir 1 is a metallic tank that was connected to a centrifugal pump and the Reservoir 2 is an transparent acrylic tank with length, height and width dimensions equals to 66.7 cm, 56 cm and 16.5 cm, respectively. A positive displacement hydrometer, previously calibrated and located on the test line, as showed in Figure 1, was used to measure and control the liquid flow in the tests. The principle of communicating vessels held both reservoirs with the same static level; this arrangement allowed to decrease turbulence effects due to suction pump. An 1 hp centrifugal pump moved fluid from Reservoir 1 to a vertical circular nozzle. The liquid jet coming from the nozzle reaches the stagnant liquid surface of the Reservoir 2, producing a turbulent kinetic energy dissipation and, consequently, entrainment of air in the liquid pool. The nozzle holder allowed to vary the height between the outlet nozzle and the liquid surface level of the Reservoir 2.

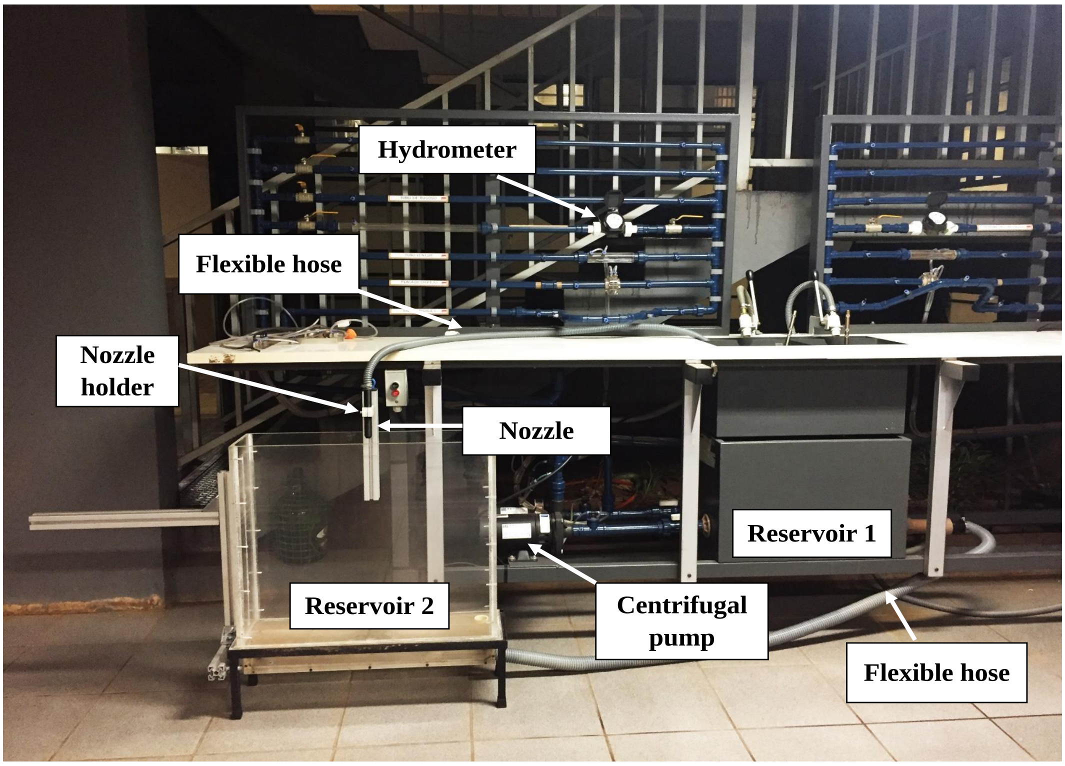

Figure 1. Experimental facility used in the present work

In the air entrainment phenomenon produced by a plunging jet system, it is recognized as main variables the output velocity (V_n), related directly with the liquid flow (Q_l), nozzle height respect to the stagnant surface (H_n), nozzle diameter (D_n) and the nozzle length (L_n). Furthermore, we must assure that the reservoir level was enough to have a complete development of the plunging jet. All these variables are well specified in Figure 2(a).

The nozzle used in this study has a length-diameter ratio $\left(\frac{L_n}{D_n}\right)$ of 17.6 to ensure a fully turbulent velocity profile inside itself, thereby maximizing the air entrainment in the liquid pool (Evans *et al.*, 1992). Figure 2(b) shows the characteristics of the nozzle designed. The nozzle was installed vertically.

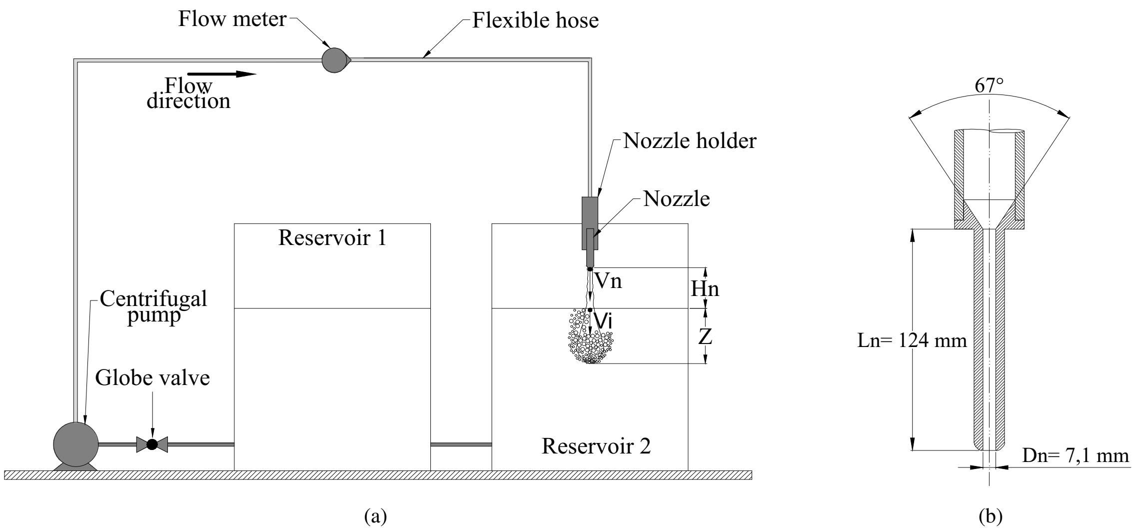

Figure 2. Facility schematic representation (a) Main variables in a plunging jet phenomenon (b) Nozzle details.

2.2 Experimental matrix

To carry out the experimental campaign, it was proposed an experimental matrix shows in Table 1. In total 15 experimental points were collected to determine the mean penetration depth. Five liquid flows with five different nozzle heights were tried so as to observe how the air entrainament phenomenon was and determine the penetration depth of the bubbles to various experimental conditions.

The liquid flow range was determined according to our experimental setup. We considered the maximum liquid flow that one where the bubble entrained did not reach the bottom of the Reservoir 2. It flow was divided into smaller flows corresponding to 40%, 60%, 80% and 100% of the maximum flow. Liquid flow of 20% were also tested but our experimental facility showed instabilities in low flows could not reach the permanent regime and consequently the results obtained were not accurate. The Nozzle heights were chosen in accordance with the quantity of air entrained and the liquid flow previously defined, ensuring that the bubbles did not hit any of the walls of the Reservoir 2, in this way, the phenomenon could be studied without disturbances.

In the present work, we did not considered variations in the Nozzle angle. More experiments will be made in order to reduce the bubble overlapping in the biphasic region and estimate the minimum bubble diameter and the kinetic energy dissipation length. The experimental points are reported in Table 1.

Table 1. Experimental matrix used in the present work.

Factor	Limits	Factors number
Inclination angle, β	90 °	1
Liquid flow, Q_l (L/min)	4.63, 6.94, 9.25 and 11.57 corresponding to 40%, 60%, 80% and 100% of the maximum liquid flow	4
Nozzle Height, H_n (cm)	5, 10, 15 and 20	4
Total experimental points		16

2.3 Data collection procedure

To collect the experimental data, we used a *planar image* and a *Shadow Sizing* techniques. So, we used a hight speed camera an a backlight so that the bubbles appear darkened in the image with a greater contrast, making the further processing of the image less susceptible to errors (Said, 2011).

Since defined the Nozzle height and the liquid flow, it was necessary to define a lens to be used in the recording. This lens was was calibrated, see Figure3(a), with a measurement standard which was located in the vertical plane in the middle of the Reservoir 2, i.e., on the vertical plane of the nozzle in order to film the central region where phenomenons, such as, breaking and coalescence bubbles take place. In our experiments, we just used an Olympus i-Speed3 camera with AF Nikkor 28 mm f/1.4D lens for all the tests. Furthermore, two LED lamps of 30 W and 2300 lumen were used for recording images with better contrast. Recording speed of either 1000 fps or 1500 fps and shutter speed x1 or x2 were chosen during the experiments to improve the bubble outlines. Figure 3(b) shows a common recording process. From a view screen could be observed the quality of the pictures and we also could change some camera settings for better image quality.

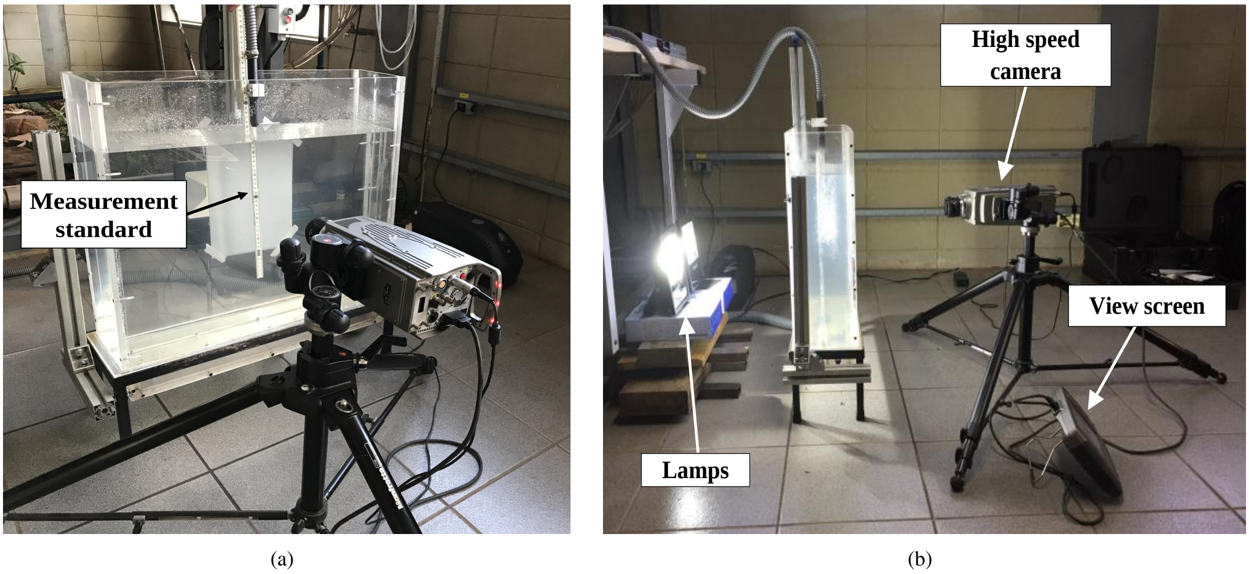

Figure 3. Data collection procedure (a) Calibration process (b) Recording process.

2.4 Processing and data analysis

The images were processed using an algorithm with filtering techniques in the Image Processing Toolbox in MatLab ® software, version R2015a. An algorithm with filtering techniques was designed so that to determine the penetration depth for each image and then the mean penetration depth. The algorithm converted the original images recorded into gray-scale and binary images. Later, we used a *imdilate* function in order to obtain the drop clearly, 2400 frames were obtained, which 48 were analyzed in each experimental point, i.e., 50 in 50 were analyzed. After this image processing stage, we calculated the penetration depth using an algorithm which works as follows:

1. Using two loops for from the bottom left, left to right and upwards, in order to find the first white pixel. This point could be the first pixel of the bubble deeper.
2. After identifying the first white pixel, the 100 pixels above that point were added and putted into a variable, white pixels have value 1 and black have value 0. If the sum were greater than 85, it means that 85% of the pixels above are white, that point represents the penetration height. Its verification avoid false detections of noise as bubbles, as a white dot or a very small bubble would not be identified as the penetration height.
3. The same previous operation was applied for the sample of 48 images, obtaining a vector with the number of pixels that represented the penetration depth obtained in each image.
4. The vectors obtained were converted to a length scale knowing the proportion of number of pixel by each 1 mm of length.
5. From the new vector of penetration depths, in length scale, we obtained the mean of the penetration and the standard deviation.

3. RESULTS

3.1 Penetration depth

After the experimental work, we could observe and study the biphasic region obtained into the Reservoir 2 due to air entrainment produced by the water jet. From the images recorded, a region of air and water with cone shape was found, as presented in Figure 4(a). We noticed a characteristic movement of the bubbles as reported in the literature, they got down following a helical path where the kinetic energy was predominant, the bubbles reached their terminal velocity and later they got the maximum penetration depth before starting to go up with an helical movement too. These results were consistent with the data reported by Ohkawa *et al.* (1987); Qu *et al.* (2011, 2013) and Harby *et al.* (2014).

The image processing carried out in order to determine the penetration depth showed values of penetration depth which depending on the liquid flow and the Nozzle height. Figure 4(d) represents the penetration depth for a common experimental point. It can be noticed that the MatLab algorithm is able to calculate the maximum penetration of the biphasic region and as we expected, this height was coincident with the vertical axis of the cone due to experimental symmetry.

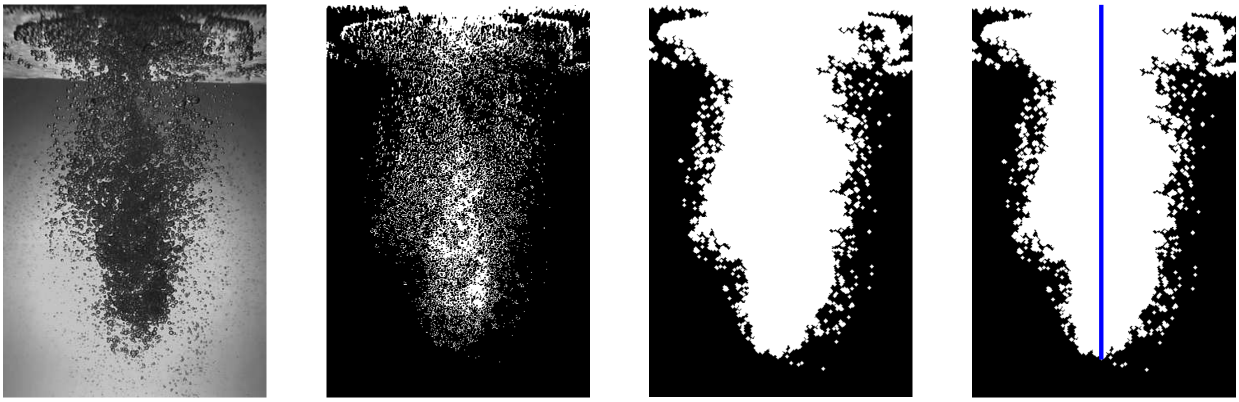

(a) (b) (c) (d)

Figure 4. Image processing considered for data analysis. (a) Grayscale image, (b) Binary image, (c) Dilated image (d) Penetration depth.

According to the experimental data, the penetration depth is related to the liquid flow and Nozzle height. It could be noticed when we compared the penetration depth for each condition reported in Table 1. It was realized that the higher flow jet (high value of impact velocity V_i), the more air entrainment. In the same way, the higher Nozzle height, the more air entrainment and less penetration depth, we show these results in Figure 5 and they were also described by Harby *et al.* (2014).

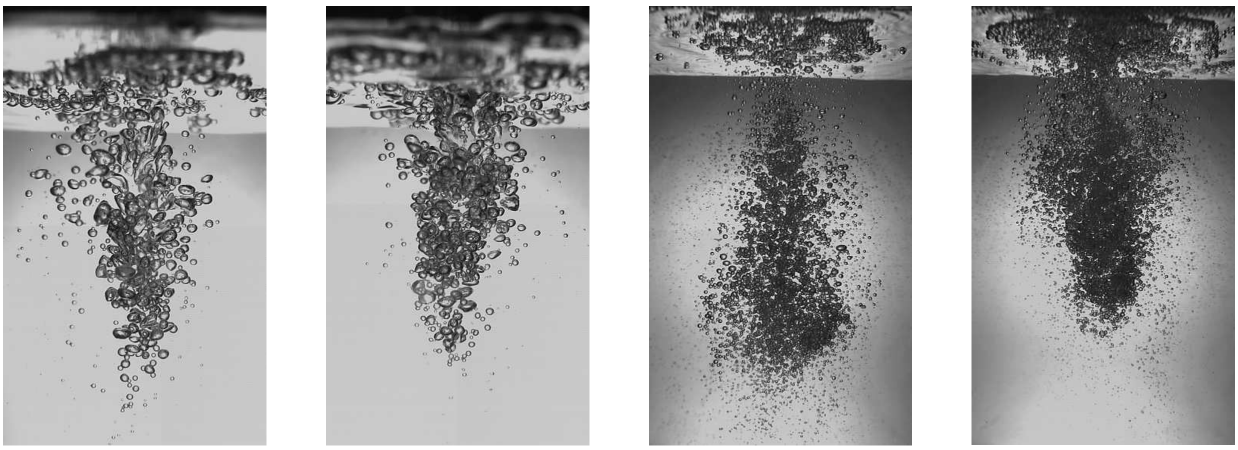

(a) (b) (c) (d)

Figure 5. Instantaneous pictures for different impact velocities and Nozzle height. (a) Q_l= 20 % L/ min, H_n=5 cm; (b) Q_l= 20 % L/ min, H_n=10 cm; (c) Q_l= 40 % L/ min, H_n=10 cm; (d) Q_l= 40 % L/ min, H_n=20 cm.

Figure 6 represents the variation of penetration depth (Z) through the liquid flow (Q_l) to different Nozzles heights (H_n) tested. It can be observe that for turbulent flows, the penetration depth increases with the liquid flow and decreases with the Nozzle height. In this work, we also made tests with low flows, Q_l= 2.31 L/ min, corresponding to 20% of the maximum liquid flow, but the water flow showed a lot of fluctuations, so we could not reach the desired system stability. This issue can be explained because of the laminar flows could have been operating in a high inaccuracy zone of the centrifugal pump, causing the system did not reach a steady state. In the other hand. In addiction, some tests with Nozzle height equal to 1.5 cm and 0 cm were performed but inconsistent results were obtained for 1.5 cm whereas with 0 cm there was not air entrainment to any liquid flow, it was due to lack of air to be dragged by the water jet.

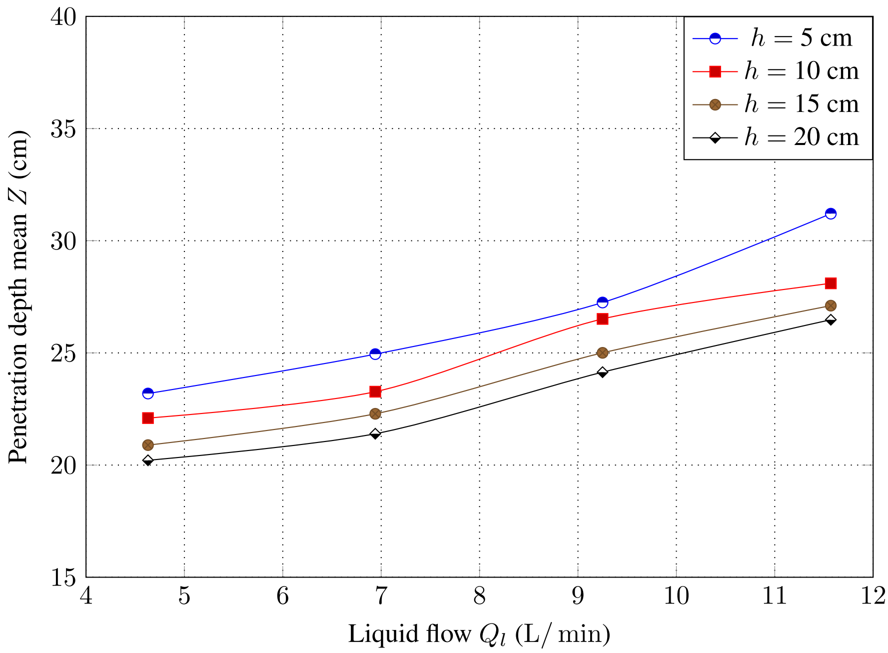

Figure 6. Penetration depth mean to different Nozzle heights

The mean penetration depths obtained for each experimental condition showed in Figure 6 are summarized in Table 2 with their respective standard deviation.

Table 2. Penetration depth mean and standard deviation for each experimental point.

	$\mathbf{Z} \pm \sigma$ (cm)			
$\mathbf{H_n}$(cm)	$\mathbf{Q_{40\%}}$	$\mathbf{Q_{60\%}}$	$\mathbf{Q_{80\%}}$	$\mathbf{Q_{100\%}}$
5.0	23.19±0.58	24.94±0.94	27.24±0.82	31.20±1.24
10.0	22.10±0.93	23.37±1.51	26.51±1.56	28.10±0.77
15.0	20.89±0.67	22.28±1.13	25.00±1.35	27.10±0.98
20.0	20.21±0.84	21.39±1.27	24.14±1.65	26.47±2.09

4. CONCLUDING REMARKS

After this experimental work we could conclude that, for turbulent flows, the air entrainment phenomenon produced by a vertical plunging jet is controlled by the liquid flow and the Nozzle height. The quantity of air entrained is related directly to the air dragged by the water jet, i.e., the higher Nozzle height, the more air entrained below the free liquid surface. Nevertheless, the penetration depth decreased when the Nozzle height increased. On the other hand, the penetration depth reached by the biphasic cone was characterized by two process of energy dissipation, breaking bubbles and coalescence; the first one takes place in the upper of the cone where the turbulence dominated the flow, whereas the second one occurs in the cone's lower region where coalescence effects between the bubbles play an important role. Finally, more experiments must be performed in order to identifying the kinetic energy dissipation length and to study the statistical distribution of bubbles in this region.

5. ACKNOWLEDGEMENTS

The authors would like to thank the PETROBRAS and FIPAI for the financial support and CNPq for the research grant.

6. REFERENCES

Biń, A.K., 1993. "Gas entrainment by plunging liquid jets". *Chemical Engineering Science*, Vol. 48, No. 21, pp. 3585–3630. ISSN 00092509. doi:10.1016/0009-2509(93)81019-R.

Bonetto, F. and Lahey, R., 1993. "An experimental study on air carryunder due to a plunging liquid jet". *International Journal of Multiphase Flow*, Vol. 19, No. 2, pp. 281–294. ISSN 03019322. doi:10.1016/0301-9322(93)90003-D.

Brattberg, T. and Chanson, H., 1998. "Air entrapment and air bubble dispersion at two-dimensional plunging water jets". *Chemical Engineering Science*, Vol. 53, No. 24, pp. 4113–4127. ISSN 00092509. doi:10.1016/S0009-2509(98)80004-3.

Bröder, D. and Sommerfeld, M., 2007. "Planar shadow image velocimetry for the analysis of the hydrodynamics in bubbly flows". *Measurement Science and Technology*, Vol. 18, No. 8, pp. 2513–2528. ISSN 0957-0233. doi:10.1088/0957-0233/18/8/028. URL http://stacks.iop.org/0957-0233/18/i=8/a=028?key=crossref.67842399811d693a0477f71d9607031d.

Burgess, J. and Molloy, N., 1973. "Gas absorption in the plunging liquid jet reactor". *Chemical Engineering Science*, Vol. 28, No. 1, pp. 183–190. ISSN 00092509. doi:10.1016/0009-2509(73)85099-7.

Celata, G.P., Cumo, M., D'Annibale, F., Di Marco, P., Tomiyama, A. and Zovini, C., 2006. "Effect of gas injection mode and purity of liquid on bubble rising in two-component systems". *Experimental thermal and fluid science*, Vol. 31, No. 1, pp. 37–53. ISSN 0894-1777.

Chanson, H., 1992. "Discussion: Reduction of cavitation on spillways by induced air entrainment". *Canadian Journal of Civil Engineering*, Vol. 19, No. 5, pp. 926–928. ISSN 0315-1468. doi:10.1139/l92-105. URL http://dx.doi.org/10.1139/l92-105.

Chanson, H. and Brattberg, T., 2000. "Experimental study of the airâĂŞwater shear flow in a hydraulic jump". *International Journal of Multiphase Flow*, Vol. 26, No. 4, pp. 583–607. ISSN 03019322. doi:10.1016/S0301-9322(99)00016-6.

Cummings, P.D. and Chanson, H., 1997. "Air Entrainment in the Developing Flow Region of Plunging JetsâĂŤPart 1: Theoretical Development". *Journal of Fluids Engineering*, Vol. 119, No. 3, pp. 597–602. ISSN 0098-2202. URL http://dx.doi.org/10.1115/1.2819286.

Evans, G., Jameson, G. and Atkinson, B., 1992. "Prediction of the bubble size generated by a plunging liquid jet bubble column". *Chemical Engineering Science*, Vol. 47, No. 13, pp. 3265–3272. ISSN 00092509. doi:10.1016/0009-2509(92)85034-9.

Harby, K., Chiva, S. and Muñoz-Cobo, J., 2014. "An experimental study on bubble entrainment and flow characteristics of vertical plunging water jets". *Experimental Thermal and Fluid Science*, Vol. 57, pp. 207–220. ISSN 08941777. doi:10.1016/j.expthermflusci.2014.04.004.

Hassan, Y.A., Ortiz-villafuerte, J. and Schmidl, W.D., 2001. "Three-dimensional measurements of single bubble dynamics in a small diameter pipe using stereoscopic particle image velocimetry". Vol. 27, pp. 817–842.

Maaß, S., Horn, S. and Kraume, M., 2008. "Measurement techniques for drop size distributions in stireed and fast coalescing liquid-liquid systems ".

Ohkawa, A., Kusabiraki, D. and Sakai, N., 1987. "Effect of Nozzle Length on Gas Entrainment Characteristics of Vertical Liquid Jet." *Journal of Chemical Engineering of Japan*, Vol. 20, No. 3, pp. 295–300. ISSN 00219592. doi:10.1252/jcej.20.295.

Qu, X.L., Khezzar, L., Danciu, D., Labois, M. and Lakehal, D., 2011. "Characterization of plunging liquid jets: A combined experimental and numerical investigation". *International Journal of Multiphase Flow*, Vol. 37, No. 7, pp. 722–731. ISSN 03019322. doi:10.1016/j.ijmultiphaseflow.2011.02.006.

Qu, X., Goharzadeh, A., Khezzar, L. and Molki, A., 2013. "Experimental characterization of air-entrainment in a plunging jet". *Experimental Thermal and Fluid Science*, Vol. 44, pp. 51–61. ISSN 08941777. doi:10.1016/j.expthermflusci.2012.05.013.

Roy, A., Maiti, B. and Das, P., 2013. "Visualisation of Air Entrainment by a Plunging Jet". *Procedia Engineering*, Vol. 56, pp. 468–473. ISSN 18777058. doi:10.1016/j.proeng.2013.03.148.

Said, M.F.b.M., 2011. *Development of Particle Sizing Based on Dynamic Image Analysis*. Ph.D. thesis, University of Leicester.

Zhang, W.h., Jiang, X. and Liu, Y.m., 2012. "A method for recognizing overlapping elliptical bubbles in bubble image". *Pattern Recognition Letters*, Vol. 33, No. 12, pp. 1543–1548. ISSN 0167-8655. doi:10.1016/j.patrec.2012.03.027. URL http://dx.doi.org/10.1016/j.patrec.2012.03.027.

7. RESPONSIBILITY NOTICE

The authors are the only responsible for the printed material included in this paper.